Published in final edited form as:
J Nucl Med. 2009 November ; 50(11): 1794–1800. doi:10.2967/jnumed.109.063743.

Using Cerebral White Matter for Estimation of Nondisplaceable Binding of 5-HT$_{1A}$ Receptors in Temporal Lobe Epilepsy

Giampiero Giovacchini[1,2], **Shielah Conant**[2], **Peter Herscovitch**[2], and **William H. Theodore**[3]

[1] Department of Nuclear Medicine, S. Andrea Hospital, La Spezia, Italy [2] PET Department, Clinical Center, National Institute of Neurological Diseases and Stroke, National Institutes of Health, Bethesda, Maryland [3] Clinical Epilepsy Section, National Institute of Neurological Diseases and Stroke, National Institutes of Health, Bethesda, Maryland

Abstract

The estimation of nondisplaceable binding from cerebellar white matter, rather than from whole cerebellum, was proposed for the PET tracer carbonyl-^{11}C-WAY-100635 (*N*-{2-[4-(2-methoxyphenyl)-1-piperazinyl]ethyl}-*N*-(2-pyridyl)cyclohexane-carboxamidel]) because of the heterogeneity of total ligand binding in this region. For the 5-hydroxytryptamine receptor 1A (5-HT$_{1A}$) antagonist ^{18}F-*N*-{2-[4-(2-methoxyphenyl)piperazin-1-yl]ethyl}-*N*-2-pyridyl)*trans*-4-fluorocyclohexanecarboxamide (^{18}F-FCWAY), the estimation of nondisplaceable binding from cerebellum (V_{ND}) may be additionally biased by spillover of ^{18}F-fluoride activity from skull. We aimed to assess the effect of using cerebral white matter as reference region on detection of group differences in 5-HT$_{1A}$ binding with PET and ^{18}F-FCWAY.

Methods—In 22 temporal lobe epilepsy patients (TLE) and 10 healthy controls, ^{18}F-FCWAY distribution volume in cerebral white matter (V_{WM}) was computed using an extrapolation method as part of a partial-volume correction (PVC) algorithm. To assess the feasibility of applying this method to clinical studies in which PVC is not performed, V_{WM} was also calculated by placing circular, 6-mm-diameter regions of interest (ROIs) in the centrum semiovalis on parametric images. Binding potentials were $BP_F = (V_T - V_{ND})/f_P$ and $BP_{F\text{-}WM} = (V_T - V_{WM})/f_P$, where V_T is total distribution volume and f_P = ^{18}F-FCWAY plasma free fraction. Statistical analysis was performed using *t* tests and linear regression.

Results—In the whole group, V_{WM} was 14% ± 19% lower than V_{ND} ($P < 0.05$). V_{WM}/f_P was significantly ($P < 0.05$) lower in patients than in controls. All significant ($P < 0.05$) reductions of 5-HT$_{1A}$ receptor availability in TLE patients detected by BP_F were also detected using $BP_{F\text{-}WM}$. Significant ($P < 0.05$) reductions of 5-HT$_{1A}$ specific binding were detected by $BP_{F\text{-}WM}$, but not BP_F, in ipsilateral inferior temporal cortex, contralateral fusiform gyrus, and contralateral amygdala. However, effect sizes were similar for $BP_{F\text{-}WM}$ and BP_F. The value of V_{WM} calculated with the ROI approach did not significantly ($P > 0.05$) differ from that calculated with the extrapolation approach (0.67 ± 0.32 mL/mL and 0.72 ± 0.34 mL/mL, respectively).

Conclusion—Cerebral white matter can be used for the quantification of nondisplaceable binding of 5-HT$_{1A}$ without loss of statistical power for detection of regional group differences. The ROI approach is a good compromise between computational complexity and sensitivity to spillover of activity, and it appears suitable to studies in which PVC is not performed. For ^{18}F-

For correspondence or reprints contact: Giampiero Giovacchini, Department of Nuclear Medicine, S. Andrea Hospital, 19124 La Spezia, Italy. giampiero.giovacchini@asl5.liguria.it.

FCWAY, this approach has the advantage of avoiding spillover of ^{18}F-fluoride activity onto the reference region.

Keywords

epilepsy; white matter; PET; 5-HT$_{1A}$ receptors; ^{18}F-FCWAY

Pet studies of serotonergic 5-hydroxytryptamine receptor 1A (5-HT$_{1A}$) are of interest in several neuropsychiatric disorders. Carbonyl-^{11}C-WAY-100635 and ^{18}F-*N*-{2-[4-(2-methoxyphenyl)piperazin-1-yl]ethyl}-*N*-2-pyridyl)*trans*-4-fluorocyclohexanecarboxamide (^{18}F-FCWAY) are frequently used for quantitative measurements with PET of 5-HT$_{1A}$ receptor specific binding. Quantification of the binding potential requires the estimation of nondisplaceable (free plus nonspecific) binding. Autoradiographic studies showed that, among gray matter regions, 5-HT$_{1A}$ receptor concentration was lowest in the cerebellum (1,2). Therefore, this region traditionally has been used for the estimation of nondisplaceable binding for 5-HT$_{1A}$ tracers.

More recently, PET studies with carbonyl-^{11}C-WAY-100635 indicated a significant concentration of 5-HT$_{1A}$ in cerebellar vermis and cortex of adult subjects and suggested that cerebellar white matter could be a better reference region for the estimation of nondisplaceable binding (3,4). The potential advantage of using cerebellar white matter has been addressed in a limited number of studies (3–5).

The possibility of using a reference region other than the cerebellum is of particular interest for the 5-HT$_{1A}$ tracer ^{18}F-FCWAY (6). After intravenous injection, this tracer rapidly undergoes defluorination to ^{18}F-fluoride, which irreversibly accumulates in the skull (7), causing substantial spillover of activity into the neighboring brain tissue. Despite the development of a correction strategy (8,9), tissue counts can be biased, especially in low-binding regions such as the cerebellum. Therefore, regions of interest (ROIs) have been drawn far from the cortical rim to avoid bias in binding potential measurement (10).

On the basis of results obtained for carbonyl-^{11}C-WAY-100635 with cerebellar white matter and because of the distance of the centrum semiovalis from the extracerebral ^{18}F-fluoride activity, we hypothesized that cerebral white matter could be a valid alternative to the cerebellum for the estimation of nondisplaceable binding for ^{18}F-FCWAY. The aim of this study was to assess the impact on detection of differences in 5-HT$_{1A}$ receptor availability between temporal lobe epilepsy (TLE) patients and healthy controls using ^{18}F-FCWAY binding in cerebral white matter as an estimate of nondisplaceable binding. The regional pattern of group differences obtained using the cerebellum was previously reported (10).

MATERIALS AND METHODS

Patient Selection

Data from 22 TLE patients (18 men; mean age ± SD, 37 ± 11 y) and 10 healthy volunteers (7 men; mean age, 35 ± 9 y) previously studied (10) were reexamined. Briefly, patients were referred for evaluation of medically refractory TLE. All patients were taking different combinations of antiepileptic drugs (10,11). None had experienced partial seizures for at least 2 d, or a secondarily generalized tonic clonic seizure for at least 1 mo, before PET studies. T1-weighted volumetric MR images were acquired for segmentation purposes, and T2-weighted and fluid-attenuated inversion recovery (FLAIR) images were obtained for the evaluation of mesial temporal sclerosis. The study was approved by the National Institute of Neurological Disorders and Stroke Institutional Review Board and the National Institutes of Health Radiation Safety Committee.

PET Procedure

Each patient was scanned with an Advance Tomograph (GE Healthcare). A bolus of 333 ± 74 MBq of ^{18}F-FCWAY was injected intravenously, and dynamic scanning was performed for 120 min in 3-dimensional mode. Arterial samples were taken to quantify plasma ^{18}F-FCWAY and ^{18}F-fluorocyclohexanecarbox-ylic acid metabolite (^{18}F-FC) concentrations and whole-blood activity. The ^{18}F-FCWAY fraction unbound to plasma proteins was measured with ultracentrifugation (12).

PET Data Analysis

Radioactivity frames registered to MR images (13) were corrected for cerebral uptake of acid radioactive metabolite, intravascular radioactivity, and ^{18}F-fluoride spillover onto the brain (8,9). The method to correct for ^{18}F-fluoride spillover assumes that there is a known true skull time–activity curve, and each brain region receives a fractional contribution of this time–activity curve that is higher for areas that are closer to the skull (8,9). Next, a previously developed partial-volume correction (PVC) algorithm (10,14) was applied. Briefly, the PVC algorithm corrects on a frame-by-frame basis gray matter pixels for spill-out of gray matter activity and for spill-in of activity from white matter (15). No correction for partial-volume averaging between adjacent gray matter regions is performed (16,17). The procedure is based on the segmentation of MR images into binary masks (18), which are subsequently smoothed to the PET resolution; these smoothed masks are named s_{GM}, s_{WM}, and s_{CSF}. The corrected activity gray matter values can be calculated as follows:

$$C_{PVC} = \frac{C_{ORIG} - C_{WM} S_{WM}}{S_{GM}}, \quad \text{Eq. 1}$$

where C_{PVC} represents the corrected activity value in a gray matter pixel after PVC, C_{ORIG} is the original uncorrected pixel value, C_{WM} is the estimated white matter activity, and s_{GM} and s_{WM} are the pixel values (range, 0–1) from the smoothed masks for gray and white matter, respectively. Original and corrected pixel data were fitted to a 2-tissue-compartment model with 3 parameters using the metabolite-corrected input function to provide parametric images of ^{18}F-FCWAY distribution volume (V).

^{18}F-FCWAY distribution volume in cerebral white matter (V_{WM}) was estimated directly on parametric images. To obtain an accurate estimate of V_{WM}, pixel values that represent 100% white matter should be used. Such pixels have a high s_{WM} value (close to the maximum value of 1) and are typically found in the centrum semiovalis. Therefore, pixels with s_{WM} values between 0.986 and 0.995 were identified. The lower threshold of 0.986 was chosen to ensure a stable fit in all patients. Potential inaccuracies in white matter estimation introduce only marginal errors in PVC-corrected gray matter values (15,19), but the effect is expected to be more important if white matter is used as the estimate of nondisplaceable binding. An anatomic constraint was applied to avoid sampling from the basal ganglia and thalamus, in which gray matter is frequently misidentified as white matter (14). Values of these pixels were then fitted as a linear function of s_{WM}, and the fitted value at $s_{WM} = 1$ was used as an estimate of nondisplaceable binding.

The extrapolation method is used for studies in which PVC is performed. To assess the feasibility of using white matter for more routine clinical studies without PVC, V_{WM} was also calculated with an ROI procedure on parametric PET images. First, 3 contiguous transverse slices for which the centrum semiovalis displayed minimal activity were identified. Next, a 6-mm ROI was centered on the area of lowest signal in both hemispheres. This operation was performed on each identified slice, using a total of 6 ROIs. The mean

pixel value was calculated in each ROI, and the 6 regional values were averaged to obtain V_{WM}.

Derivation of Binding Potential

Binding potentials were derived using both V_{ND} and V_{WM}, as following:

$$BP_F=[(V_T - V_{ND})/f_P)], \quad \text{Eq. 2}$$

$$BP_{F-WM}=[(V_T - V_{WM})/f_P)], \quad \text{Eq. 3}$$

where V_T is the total distribution volume in the target ROI, V_{ND} is the distribution volume in the cerebellum, and f_P is ^{18}F-FCWAY plasma free fraction (20).

ROI Analysis

Temporal and extratemporal ROIs were drawn on MR images and applied to coregistered parametric images (10). Cerebellar ROIs were initially drawn along the outer cortical edge, then uniformly shrunk until, on visual inspection, no spillover of activity was observed. Final cerebellar ROIs were about 50% smaller than original ROIs (10). ROI measurements were computed using only gray matter pixels, as defined by the gray matter segment (18). For the cerebellum, for which gray matter segment definition is not accurate, the mean ROI value was computed from unmasked PET images coregistered to MRI volumes (10). The effect size was computed as the difference between patients and controls divided by the SD in the control group. Statistical analysis was performed using *t* test and linear regression, and statistical significance was set at uncorrected $P < 0.05$.

RESULTS

Figure 1 shows transverse images of ^{18}F-FCWAY distribution volume in a TLE patient. In the cerebellum, the large spillover of ^{18}F-fluoride activity masks the visualization of possible differences in specific binding between gray and white matter. At the cortical level, there is a clear difference in ^{18}F-FCWAY binding between centrum semiovalis white matter and gray matter or mixed gray matter–white matter regions. Spillover of ^{18}F-fluoride activity is observed in the left frontal and bilateral parietal cortex.

Figure 2 shows representative time–activity curves from a healthy control. In white matter, activity peaked at about 5 min after injection, then progressively decreased to 57%, 24%, and 21% of peak at 30, 60, and 120 min, respectively. The activity peak in white matter was about 40% lower than that in cerebellum. White matter and cerebellar time–activity curves overlapped, starting from about 25 min after injection. As expected, in both regions the time–activity curve was markedly different from the time–activity curve of the mesial temporal cortex.

Figure 3 shows the extrapolation method used to automatically estimate V_{WM}, as part of the PVC process. On the distribution volume images, values of voxels with smoothed white matter mask s_{WM} between 0.986 and 0.995 were fitted to a straight line, and the extrapolated value for $s_{WM} = 1$ was taken as an estimate of nondisplaceable binding. The volume of white matter voxels with an s_{WM} between 0.986 and 0.995 was 19 ± 5 mL. The quality of fit, as quantified by r^2 values, was good in the whole sample ($r^2 = 0.88 \pm 0.11$; range, 0.59–0.99).

In the whole sample, V_{WM} estimated with the extrapolation approach was significantly smaller than V_{ND} (0.72 ± 0.34 mL/mL and 0.84 ± 0.30 mL/mL; paired *t* test, $P < 0.05$). The percentage difference between V_{WM} and V_{ND} was 14% ± 19%, without significant ($P > 0.05$) differences between TLE patients and controls. On a subject-by-subject basis, V_{WM} was lower or of the same magnitude as V_{ND} in all but 3 subjects, in whom V_{WM} was 11%, 14%, and 29% higher than V_{ND}. A significant relationship was found between V_{WM} and V_{ND} (regression equation, $V_{WM} = -0.10 + 0.99 \cdot V_{ND}$ [$r^2 = 0.76$; $P < 0.05$]) (Fig. 4). V_{WM} was significantly ($P < 0.05$) higher in patients than in controls (0.81 ± 0.35 mL/mL and 0.55 ± 0.25 mL/mL, respectively). ^{18}F-FCWAY f_P was significantly higher in patients than in controls (0.121 ± 0.033 vs. 0.066 ± 0.024, respectively; $P < 0.05$), a finding that may be attributed to antiepileptic drugs (10,11). V_{WM}/f_P, however, was significantly ($P < 0.05$) lower in patients than in controls (6.80 ± 2.56 mL/mL and 9.32 ± 3.16 mL/mL, respectively).

The variability of V_{WM}, as quantified by the percentage coefficient of variation (%CV), was greater than that of V_{ND} (45.2% vs. 39.5% in controls and 43.0% vs. 31.6% in patients, respectively). Nevertheless, the variability of $BP_{F\text{-}WM}$ was not significantly higher ($P > 0.05$) than that of BP_F, respectively. In the whole group, mean values of %CV across ROIs were 36.8% ± 5.6 and 35.5% ± 6.0, respectively, for BP_F and $BP_{F\text{-}WM}$.

All significant differences detected using BP_F (10) were also detected using $BP_{F\text{-}WM}$. Significantly ($P < 0.05$) lower $BP_{F\text{-}WM}$, but not BP_F, was detected in ipsilateral inferior temporal cortex, contralateral fusiform gyrus, and contralateral amygdala. However, effect sizes were similar for $BP_{F\text{-}WM}$ and BP_F (Table 1).

In the whole group, values of V_{WM} calculated with the ROI approach did not significantly differ from those obtained with the extrapolation technique (0.67 ± 0.32 mL/mL and 0.72 ± 0.34 mL/mL, respectively; $P > 0.05$). Group differences in specific binding were detected without any regional discrepancy in comparison to those detected with the extrapolation approach.

DISCUSSION

The cerebellum has been used in several PET studies to estimate nondisplaceable binding of 5-HT_{1A}. However, for both carbonyl-^{11}C-WAY-100635 (21–23) and ^{18}F-FCWAY (8), a 2-compartment model was necessary to accurately fit cerebellar time–activity curves. This finding was attributed to a slow component of nondisplaceable binding or to the progressive accumulation of radioactive metabolites (8,21–23). This unexpected finding motivated the search for nontraditional reference regions for the estimation of non-displaceable binding.

Using PET with carbonyl-^{11}C-WAY-100635, Parsey et al. found that cerebellar white matter time–activity curves were well described by a 1-tissue-compartment model (3). Using cerebellar white matter, rather than the whole cerebellum, for the derivation of the binding potential improved the identifiability and time stability in all cortical regions. The authors concluded that for carbonyl-^{11}C-WAY-100635, cerebellar white matter could be a better reference region than the whole cerebellum (3).

For ^{18}F-FCWAY, the estimation of nondisplaceable binding from the cerebellum has the additional problem of spillover of ^{18}F-fluoride activity. This applies to the cortex as well, even though specific binding is high in cortical regions. A method to correct for such spillover was developed. This method, however, does not accurately take into account intersubject variations in the skull shape and thickness (8,9). Disulfiram was used to inhibit defluorination of ^{18}F-FCWAY in humans (24). The drug reduced the accumulation of ^{18}F-fluoride in the skull and improved the visualization of radioligand cerebral binding.

However, disulfiram also affected the clearance of ^{18}F-FCWAY and acid radioactive metabolite and jeopardized the accuracy of the compartmental analysis (24).

A simple approach to minimize the effect of ^{18}F-fluoride spillover onto the cerebellum is to draw ROIs far from the cerebellar edge (10). However, some residual spillover from the bone or mixing of regions with different 5-HT$_{1A}$ receptor concentrations cannot be excluded. Alternatively, a different reference region could be identified.

Suitability of Cerebral White Matter for Quantification of ^{18}F-FCWAY Nondisplaceable Binding

The suitability of a region to provide an estimate of nondisplaceable binding can be inferred from kinetic analysis or preblocking studies. Adequate fitting with a 1-tissue-compartment model and negligible k_3 and k_4 values are consistent with a lack of significant concentration of specific receptors. In preblocking studies, the baseline regional distribution volume is compared with that obtained after the administration of a specific receptor cold ligand. If a region is truly devoid of specific binding, the regional value should be comparable in the 2 conditions. Carson et al. performed preblocking ^{18}F-FCWAY PET studies in monkeys (8). The administration of unlabelled WAY-100635 in advance produced a significant reduction in total binding in the cerebellum by about 44%. This result is inconsistent with the assumption that the cerebellum is a region with only nondisplaceable binding sites for ^{18}F-FCWAY. Unfortunately, changes of the distribution volumes in white matter were not evaluated (8). Admittedly, the lack of preblocking studies and of formal kinetic analysis, that is, analysis of goodness of fit and calculation of rate constants, represents a significant limit of this study.

Cerebral white matter would be expected to be suitable for the quantification of nondisplaceable binding. White matter is composed of bundles of myelinated axons. The myelin sheath, which is produced by glial cells, is a bimolecular layer of lipids interspersed between protein layers. No significant expression of 5-HT$_{1A}$ or receptor messenger RNA was found in glial cells (25–27).

Visual inspection of both carbonyl-^{11}C-WAY-100635 (3,28) and ^{18}F-FCWAY (8,10,24) images shows low activity in the centrum semiovalis.

Finally, starting from about 25 min after the injection of ^{18}F-FCWAY, the cerebral white matter time–activity curve is similar to the cerebellar time–activity curve, and both time–activity curves have characteristics consistent with negligible concentration of specific binding sites, compared with the cortex.

Group Differences Using White Matter

We failed to show a substantial gain in statistical power using white matter. In TLE patients, lower 5-HT$_{1A}$ receptor specific binding was detected in ipsilateral inferior temporal cortex, contralateral fusiform gyrus, and contralateral amygdala using V_{WM} but not V_{ND} (Table 1). However, by comparing P values and effect sizes, it is evident that the lack of significant group differences in these regions using BP_F (10) is likely a false-negative finding. These results are not unexpected given that regional values of specific binding are much greater than those of nondisplaceable binding, independently of the reference region. Our findings are consistent with results obtained with carbonyl-^{11}C-WAY-100635, indicating no substantial advantage in the detection of sex differences in the hippocampus using $BP_{F\text{-}WM}$, compared with using BP_F (3).

Comparison Between V_{WM} and V_{ND}

We found lower V_{WM} than V_{ND}. Although this difference was statistically significant, the magnitude of the difference (14%) was low, and several factors could contribute to this finding. Admittedly, smaller ^{18}F-FCWAY distribution volume in white matter per se does not constitute evidence of less specific binding. Because of the low parent accumulation in these regions, differences in radioligand delivery, blood volume, radiometabolite accumulation, spillover of ^{18}F-fluoride onto the cerebellum, and partial-volume averaging could contribute to this difference.

The lower peak of the white matter time–activity curve than of the cerebellar time–activity curve likely reflects lower flow-mediated radioligand delivery. The lower peak of the cerebellar white matter time–activity curve than of the whole cerebellum time–activity curve was reported by Parsey et al. (3) and by Hirvonen et al. (4). Starting from about 25 min after injection, the 2 time–activity curves had similar height and time dependence.

Group Differences in Nondisplaceable Binding

The absence of significant group differences in non-displaceable binding is a prerequisite for determining that measured differences of interest reflect only specific binding. Such differences can be assessed only in arterial line–based models, which are now favored less than less invasive reference tissue models (21,29–32). However, when arterial line–based models were used, significant group differences in nondisplaceable binding with 5-HT$_{1A}$ tracers were reported. A higher V_{ND} (not corrected for f_p) was found in healthy women than in healthy men (3,33), whereas a lower uncorrected V_{ND} was found in depressed patients than in healthy controls (5). A lower V_{ND}, after correction for f_p, was previously reported in these TLE patients (10,11). If a region is devoid of specific binding and f_p drives the kinetics of the tracer, group differences in nondisplaceable binding estimates might be expected in values uncorrected for f_p, but they should be canceled out after f_p correction. These group differences could be attributed to actual differences in 5-HT$_{1A}$ receptor availability, nondisplaceable binding, blood volume, or acid corrections. For ^{18}F-FCWAY, an additional artificial cause might be the spillover of ^{18}F-fluoride activity.

Choice of Binding Outcome

Previous PET studies with carbonyl-^{11}C-WAY-100635 found that BP_F is the most sensitive binding outcome for the accurate quantification of 5-HT$_{1A}$ receptor availability (3,5,23,33). On the basis of this finding and to account for group differences in V_{ND}, we had chosen BP_F as primary binding outcome (10,11). For ^{18}F-FCWAY, the magnitude of nondisplaceable binding is small, as evidenced by the low value of V_{ND} or V_{WM}, compared with V_T, in cortical and limbic areas. Thus, V_T primarily reflects specific binding. In this sample, regional group differences detected with BP_F were similar to those detected with V_T/f_p without significant loss of statistical power (data not shown). Thus, if spillover of ^{18}F-fluoride onto the cerebellum is a concern and scientific evidence supporting the use of white matter as an estimate of nondisplaceable binding is not sufficient, the small group differences in nondisplaceable binding could be neglected and V_T/f_p could be used as primary binding outcome in future studies in TLE patients with ^{18}F-FCWAY (34).

Variability of V_{WM}

The variability of V_{WM} was higher than that of V_{ND}. Comparable %CV for cerebellar white matter and whole cerebellum was detected by both Parsey et al. (3,33) and Hirvonen et al. (4). Because of the higher specific binding of cortical regions and large interregion variability, ultimately no variability is added to ^{18}F-FCWAY binding potential measurements.

Cerebellum and TLE

In TLE patients, the use of cerebral white matter as reference region may be preferable because of cerebellar atrophy. Epilepsy itself—and some antiepileptic drugs, particularly phenytoin—may induce cerebellar structural change and hypometabolism on ^{18}F-FDG PET (35,36). These effects may be more severe in patients with long epilepsy duration and uncontrolled seizures, who are most likely to have PET studies (35). Moreover, changes in 5-HT concentration in the cerebellum have been reported because of antiepileptic drugs and the effects of uncontrolled epilepsy itself (37).

CONCLUSION

Using cerebral white matter, rather than the cerebellum, as an estimate of ^{18}F-FCWAY nondisplaceable binding, we found regional reductions of 5-HT$_{1A}$ receptor specific binding in TLE patients, without loss of statistical power. These findings add to results obtained with carbonyl-^{11}C-WAY-100635 that support the use of white matter for the estimation of nondisplaceable binding for 5-HT$_{1A}$ tracers in clinical studies and expand the emerging topic of non-traditional reference regions.

Acknowledgments

We thank Richard Carson for helpful comments and Charles Fraser for technical assistance.

References

1. Hall H, Lundkvist C, Halldin C, et al. Autoradiographic localization of 5-HT$_{1A}$ receptors in the post-mortem human brain using [^{3}H]WAY-100635 and [^{11}C]WAY-100635. Brain Res. 1997; 745:96–108. [PubMed: 9037397]
2. Burnet PW, Eastwood SL, Harrison PJ. [^{3}H]WAY-100635 for 5-HT$_{1A}$ receptor autoradiography in human brain: a comparison with [^{3}H]8-OH-DPAT and demonstration of increased binding in the frontal cortex in schizophrenia. Neurochem Int. 1997; 30:565–574. [PubMed: 9152998]
3. Parsey RV, Arango V, Olvet DM, Oquendo MA, Van Heertum RL, John Mann J. Regional heterogeneity of 5-HT$_{1A}$ receptors in human cerebellum as assessed by positron emission tomography. J Cereb Blood Flow Metab. 2005; 25:785–793. [PubMed: 15716853]
4. Hirvonen J, Kajander J, Allonen T, Oikonen V, Nagren K, Hietala J. Measurement of serotonin 5-HT$_{1A}$ receptor binding using positron emission tomography and [carbonyl-^{11}C]WAY-100635: considerations on the validity of cerebellum as a reference region. J Cereb Blood Flow Metab. 2007; 27:185–195. [PubMed: 16685258]
5. Hirvonen J, Karlsson H, Kajander J, et al. Decreased brain serotonin 5-HT1A receptor availability in medication-naive patients with major depressive disorder: an in-vivo imaging study using PET and [carbonyl-11C]WAY-100635. Int J Neuropsychopharmacol. 2008; 11:465–476. [PubMed: 17971260]
6. Lang L, Jagoda E, Schmall B, et al. Development of fluorine-18-labeled 5-HT$_{1A}$ antagonists. J Med Chem. 1999; 42:1576–1586. [PubMed: 10229627]
7. Hawkins RA, Choi Y, Huang SC, et al. Evaluation of the skeletal kinetics of fluorine-18-fluoride ion with PET. J Nucl Med. 1992; 33:633–642. [PubMed: 1569473]
8. Carson RE, Lang L, Watabe H, et al. PET evaluation of [^{18}F]FCWAY, an analog of the 5-HT$_{1A}$ receptor antagonist, WAY-100635. Nucl Med Biol. 2000; 27:493–497. [PubMed: 10962257]
9. Carson RE, Wu Y, Lang L, et al. Brain uptake of the acid metabolites of F-18-labeled WAY 100635 analogs. J Cereb Blood Flow Metab. 2003; 23:249–260. [PubMed: 12571456]
10. Giovacchini G, Toczek MT, Bonwetsch R, et al. 5-HT$_{1A}$ receptors are reduced in temporal lobe epilepsy after partial volume correction. J Nucl Med. 2005; 46:1128–1135. [PubMed: 16000281]
11. Theodore WH, Giovacchini G, Bonwetsch R, et al. The effect of antiepileptic drugs on 5-HT-receptor binding measured by positron emission tomography. Epilepsia. 2006; 47:499–503. [PubMed: 16529612]

12. Carson RE, Channing MA, Blasberg RG, et al. Comparison of bolus and infusion methods for receptor quantitation: application to [^{18}F]cyclofoxy and positron emission tomography. J Cereb Blood Flow Metab. 1993; 13:24–42. [PubMed: 8380178]
13. Jenkinson M, Smith S. A global optimisation method for robust affine registration of brain images. Med Image Anal. 2001; 5:143–156. [PubMed: 11516708]
14. Giovacchini G, Lerner A, Toczek MT, et al. Brain incorporation of [^{11}C]arachidonic acid, blood volume, and blood flow in healthy aging: a study with partial volume correction. J Nucl Med. 2004; 45:1471–1479. [PubMed: 15347713]
15. Muller-Gartner HW, Links JM, Prince JL, et al. Measurement of radiotracer concentration in brain gray matter using positron emission tomography: MRI-based correction for partial volume effects. J Cereb Blood Flow Metab. 1992; 12:571–583. [PubMed: 1618936]
16. Labbe C, Froment JC, Kennedy A, Ashburner J, Cinotti L. Positron emission tomography metabolic data corrected for cortical atrophy using magnetic resonance imaging. Alzheimer Dis Assoc Disord. 1996; 10:141–170. [PubMed: 8876777]
17. Rousset OG, Ma Y, Evans AC. Correction for partial volume effects in PET: principle and validation. J Nucl Med. 1998; 39:904–911. [PubMed: 9591599]
18. Pham DL, Prince JL. Adaptive fuzzy segmentation of magnetic resonance images. IEEE Trans Med Imaging. 1999; 18:737–752. [PubMed: 10571379]
19. Meltzer CC, Kinahan PE, Greer PJ, et al. Comparative evaluation of MR-based partial-volume correction schemes for PET. J Nucl Med. 1999; 40:2053–2065. [PubMed: 10616886]
20. Innis RB, Cunningham VJ, Delforge J, et al. Consensus nomenclature for in vivo imaging of reversibly binding radioligands. J Cereb Blood Flow Metab. 2007; 27:1533–1539. [PubMed: 17519979]
21. Gunn RN, Lammertsma AA, Hume SP, Cunningham VJ. Parametric imaging of ligand-receptor binding in PET using a simplified reference region model. Neuroimage. 1997; 6:279–287. [PubMed: 9417971]
22. Farde L, Ito H, Swahn CG, Pike VW, Halldin C. Quantitative analyses of carbonyl-carbon-11-WAY-100635 binding to central 5-hydroxytryptamine-1A receptors in man. J Nucl Med. 1998; 39:1965–1971. [PubMed: 9829590]
23. Parsey RV, Slifstein M, Hwang DR, et al. Validation and reproducibility of measurement of 5-HT_{1A} receptor parameters with [carbonyl-^{11}C]WAY-100635 in humans: comparison of arterial and reference tissue input functions. J Cereb Blood Flow Metab. 2000; 20:1111–1133. [PubMed: 10908045]
24. Ryu YH, Liow JS, Zoghbi S, et al. Disulfiram inhibits defluorination of [^{18}F]FCWAY, reduces bone radioactivity, and enhances visualization of radio-ligand binding to serotonin 5-HT_{1A} receptors in human brain. J Nucl Med. 2007; 48:1154–1161. [PubMed: 17574977]
25. Burnet PW, Eastwood SL, Lacey K, Harrison PJ. The distribution of 5-HT1A and 5-HT2A receptor mRNA in human brain. Brain Res. 1995; 676:157–168. [PubMed: 7796165]
26. Gerard C, Langlois X, Gingrich J, et al. Production and characterization of polyclonal antibodies recognizing the intracytoplasmic third loop of the 5-hydroxytryptamine1A receptor. Neuroscience. 1994; 62:721–739. [PubMed: 7870302]
27. Hall MD, el Mestikawy S, Emerit MB, Pichat L, Hamon M, Gozlan H. [^{3}H]8-hydroxy-2-(di-*n*-propylamino)tetralin binding to pre- and postsynaptic 5-hydroxytryptamine sites in various regions of the rat brain. J Neurochem. 1985; 44:1685–1696. [PubMed: 3157780]
28. Andree B, Halldin C, Pike VW, Gunn RN, Olsson H, Farde L. The PET radioligand [carbonyl-^{11}C]desmethyl-WAY-100635 binds to 5-HT_{1A} receptors and provides a higher radioactive signal than [carbonyl-^{11}C]WAY-100635 in the human brain. J Nucl Med. 2002; 43:292–303. [PubMed: 11884487]
29. Hume SP, Myers R, Bloomfield PM, et al. Quantitation of carbon-11-labeled raclopride in rat striatum using positron emission tomography. Synapse. 1992; 12:47–54. [PubMed: 1411963]
30. Lammertsma AA, Hume SP. Simplified reference tissue model for PET receptor studies. Neuroimage. 1996; 4:153–158. [PubMed: 9345505]

31. Logan J, Fowler JS, Volkow ND, Wang GJ, Ding YS, Alexoff DL. Distribution volume ratios without blood sampling from graphical analysis of PET data. J Cereb Blood Flow Metab. 1996; 16:834–840. [PubMed: 8784228]

32. Ichise M, Cohen RM, Carson RE. Noninvasive estimation of normalized distribution volume: application to the muscarinic-2 ligand [^{18}F]FP-TZTP. J Cereb Blood Flow Metab. 2008; 28:420–430. [PubMed: 17653129]

33. Parsey RV, Oquendo MA, Simpson NR, et al. Effects of sex, age, and aggressive traits in man on brain serotonin 5-HT$_{1A}$ receptor binding potential measured by PET using [C-11]WAY-100635. Brain Res. 2002; 954:173–182. [PubMed: 12414100]

34. Toczek MT, Carson RE, Lang L, et al. PET imaging of 5-HT$_{1A}$ receptor binding in patients with temporal lobe epilepsy. Neurology. 2003; 60:749–756. [PubMed: 12629228]

35. Sandok EK, O'Brien TJ, Jack CR, So EL. Significance of cerebellar atrophy in intractable temporal lobe epilepsy: a quantitative MRI study. Epilepsia. 2000; 41:1315–1320. [PubMed: 11051128]

36. Theodore WH, Fishbein D, Dietz M, Baldwin P, Deitz M. Complex partial seizures: cerebellar metabolism. Epilepsia. 1987; 28:319–323. [PubMed: 3497801]

37. Meshkibaf MH, Subhash MN, Lakshmana KM, Rao BS. Effect of chronic administration of phenytoin on regional monoamine levels in rat brain. Neurochem Res. 1995; 20:773–778. [PubMed: 7477669]

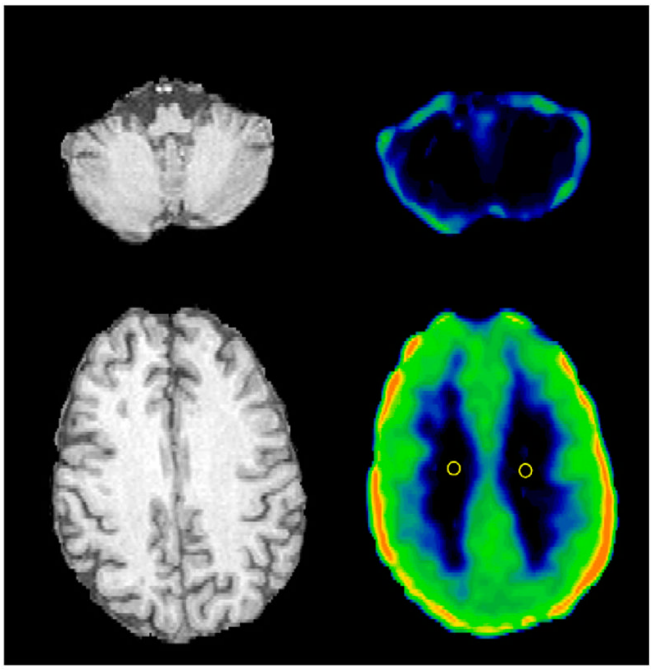

FIGURE 1.
Transverse MR and ^{18}F-FCWAY distribution volume images passing through centrum semiovalis and cerebellum in TLE patient. Negligible binding of tracer in cerebellar white matter and centrum semiovalis and large spillover of ^{18}F-fluoride activity onto cerebellum were observed. Two 6-mm-diameter, circular ROIs used for calculation of V_{WM} with manual approach are displayed. ^{18}F-FCWAY distribution volume image (V/f_P) is scaled to maximum of 80 mL/mL.

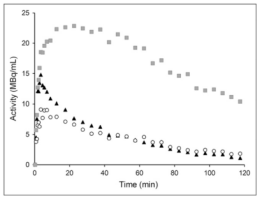

FIGURE 2.
Representative time–activity curves from healthy control for white matter (○, 1.9 cm^2), cerebellum (▲, 4.2 cm^2), and mesial temporal cortex (■, 2.8 cm^2).

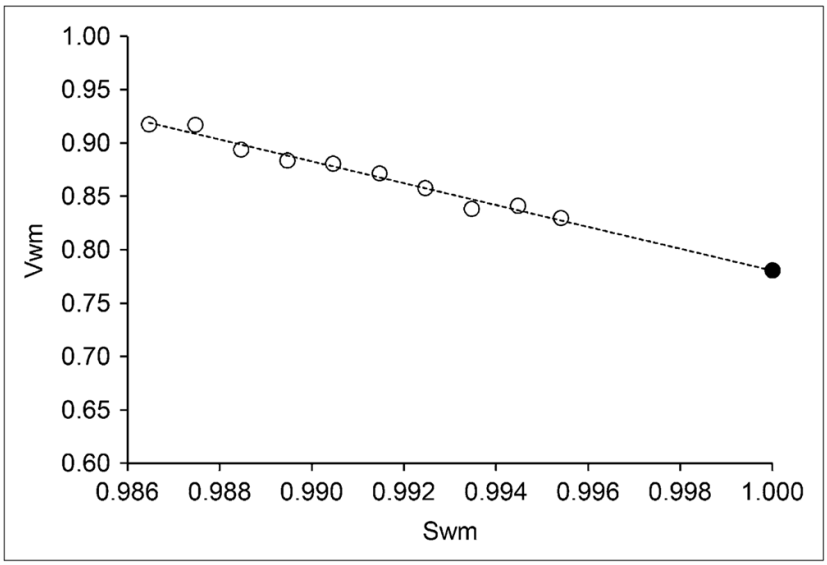

FIGURE 3.

Estimation of ^{18}F-FCWAY distribution volume in white matter (V_{WM}) with extrapolation method. Values for V_{WM} are plotted vs. smoothed white matter mask (s_{WM}). V_{WM} values of voxels with s_{WM} between 0.986 and 0.995 (○) were fitted to straight line, and value at s_{WM} = 1.0 (●) was used as estimate of nondisplaceable binding.

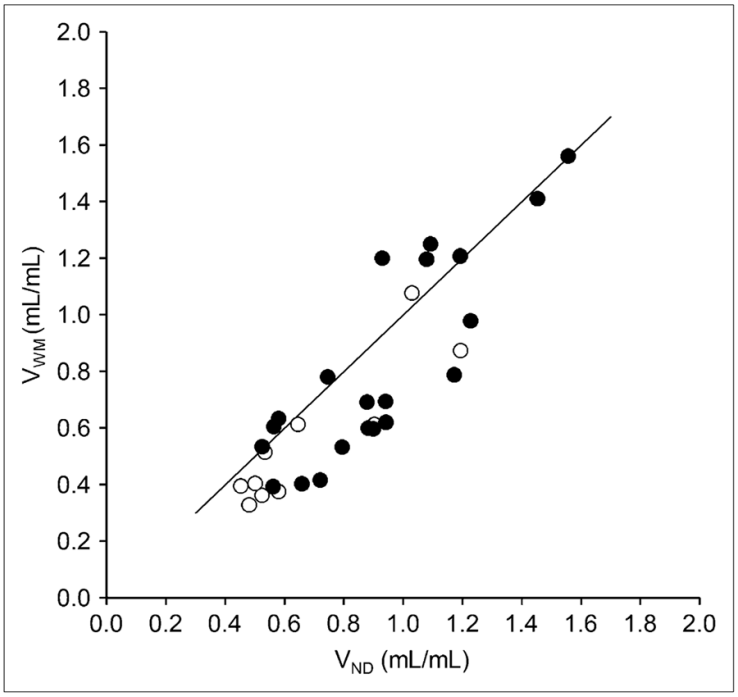

FIGURE 4.

Correlation between ^{18}F-FCWAY distribution volume in white matter (V_{WM}) and in cerebellum (V_{ND}) in controls (○) and in TLE patients (●). For whole group, regression equation was $V_{WM} = -0.10 + 0.99 \cdot V_{ND}$ ($r^2 = 0.76$; $P < 0.05$).

TABLE 1

Group Differences Detected with $BP_{F\text{-}WM}$ and BP_F

	$BP_{F\text{-}WM}$ (mL/mL)			BP_F (mL/mL)*		
Region	**Controls**	**Patients**	***P***	**Effect size**	***P***	**Effect size**
I. sup. temporal	90 ± 26	77 ± 32	0.214	−0.53	0.280	−0.50
C. sup. temporal	86 ± 24	74 ± 27	0.199	−0.52	0.264	−0.49
I. mid. temporal	97 ± 28	80 ± 29	0.113	−0.60	0.154	−0.57
C. mid. temporal	93 ± 24	78 ± 25	0.096	−0.65	0.135	−0.63
I. inf. temporal	103 ± 29	80 ± 28	0.034	−0.78	0.052	−0.76
C. inf. temporal	100 ± 26	91 ± 32	0.423	−0.32	0.528	−0.29
I. fusiform	128 ± 35	82 ± 24	<0.001	−1.35	<0.001	−1.34
C. fusiform	122 ± 32	97 ± 32	0.041	−0.78	0.058	−0.76
I. parahippocampus	146 ± 38	84 ± 26	<0.001	−1.62	<0.001	−1.62
C. parahippocampus	146 ± 42	103 ± 29	0.002	−1.02	0.003	−1.02
I. hippocampus	129 ± 29	66 ± 31	<0.001	−2.20	<0.001	−2.22
C. hippocampus	126 ± 34	99 ± 30	0.025	−0.79	0.035	−0.78
I. amygdala	75 ± 17	51 ± 20	0.002	−1.39	0.005	−1.37
C. amygdala	77 ± 16	62 ± 22	0.045	−0.94	0.078	−0.89
I. insula	97 ± 28	64 ± 21	0.001	−1.18	0.001	−1.17
C. insula	97 ± 27	67 ± 20	0.001	−1.11	0.002	−1.10
I. frontal	70 ± 18	68 ± 23	0.643	−0.16	0.820	−0.11
C. frontal	67 ± 17	64 ± 23	0.648	−0.16	0.828	−0.11
I. parietal	65 ± 18	65 ± 22	0.914	0.01	0.890	0.06
C. parietal	64 ± 18	68 ± 24	0.761	0.20	0.593	0.26
I. occipital	41 ± 11	45 ± 13	0.524	0.39	0.298	0.51
R. occipital	39 ± 8	47 ± 16	0.235	1.02	0.130	1.10

*Values obtained using V_{ND} as estimate of nondisplaceable binding (10).

I. = ipsilateral to focus; sup. = superior; C. = contralateral to focus; mid. = middle; inf. = inferior.